Civil Engineering Infrastructures Journal xx,xx

DOI: 10.22059/ceij.2025.398909.2350

Behavioral Analysis of Reinforced Concrete Deep Beams under Dynamic Loading with Varying Strain Rates Using the Strut-and-Tie Model Framework

Authors: Salehi, P., Aghayari, R., and Fazeli Kelareh, M.R

Affiliations:

Salehi, P
M.Sc. Graduate, Department of Civil Engineering, Faculty of Engineering, Razi University, Kermanshah, Iran.
Email: parsasalehi3189@gmail.com
ORCID: [https://orcid.org/0009-0004-9901-4337]

Aghayari, R
Associate Professor., Faculty of Civil Engineering of Razi University, Kermanshah, Iran.
Email: Reza_agh@razi.ac.ir
ORCID: [https://orcid.org/0000-0002-9747-3810]

Fazeli Kelareh, M.R
Ph.D. Student of Structural Engineering, Department of Civil Engineering, Faculty of Engineering, Razi University, Kermanshah, Iran.
Email: mohammadrezafazelikelareh@gmail.com
ORCID: [https://orcid.org/ 0000-0002-6745-5128]

Corresponding author: Aghayari, R
Associate Professor., Faculty of Civil Engineering of Razi University, Kermanshah, Iran.
Email: Reza_agh@razi.ac.ir

Received: 19/07/2025
Revised: 28/09/2025
Accepted: 03/10/2025

Abstract

The structural behavior of beams is central to concrete structural engineering. Deep beams have a higher height-to-span ratio than conventional beams and therefore behave differently, which makes traditional analysis and design methods inapplicable. Specialized approaches are required for effective analysis and design. One widely used technique is the strut-and-tie model (STM), which provides a reliable framework for understanding deep-beam behavior. In this study, the behavior of reinforced concrete (RC) deep beams under static and dynamic two-point loading was investigated using the finite element method (FEM) in ABAQUS within the STM framework. The analysis covered dynamic strain rates associated with vehicle-induced effects, from quasi-static to high-rate conditions. The study compared numerical results with shear capacities from a simplified STM-based formulation for static loading previously proposed by the author. Building on this method and incorporating the dynamic amplification factor (D_1, defined as the ratio of dynamic to static shear capacity), an approximate equation was developed to predict the concrete strength reduction factor for deep beams under dynamic two-point loading. The equation achieved approximately 99% accuracy and provides a practical basis for designing deep beams under dynamic loads.

Keywords: *Reinforced concrete deep beam, Dynamic Loading, Strain Rate, Strut and tie model*

1. Introduction

Reinforced concrete (RC) deep beams are critical structural components commonly used as transfer girders in foundations, offshore structures, high-rise buildings, and other applications (Kasilingam and Khanna., 2024; Fathi et al., 2021; Pouyani et al., 2024; Kaveh et al., 2021; Mohammadi Zadeh et al., 2023). The strut-and-tie method (STM) is a widely used approach for the analysis and design of deep beams and offers an effective solution to their complex behavior (CEN., 2004; ISBN., 2010). Ritter (1899) first introduced the truss concept for shear design in flexural concrete members. Morsch (1909) later refined the model, arguing that diagonal compressive stresses in concrete form a continuous field in equilibrium with stirrup forces rather than discrete zones. Interest in STM renewed in the 1980s, with researchers such as Collins and Mitchell (1986) and Ramirez and Breen (1991) using truss models and plasticity theory to predict the combined effects of shear, bending, and torsion, which led to the modified compression field theory (MCFT). Schlaich and Schaffer (1991) further advanced STM by formalizing its use as a design and analytical tool for disturbed regions (D-regions) and providing practical guidelines that underpin its contemporary application. Subsequent studies expanded STM for D-regions (Abdul-

Razzaq et al., 2021; Aguilar et al., 2022; Arabzadeh et al., 2020; Megahed., 2024; Hussein and Abbas., 2022; Kondalraj and Rao., 2022; Abreu et al., 2024; Mabrouk et al., 2022; Megahed., 2024; Thomas and Ramadass., 2022; Sakalauskas and Kaklauskas., 2023; Yi et al., 2022; Mohammadi Rad et al., 2023). Using STM, Arabzadeh et al. (2009) proposed a method for the shear capacity of simply supported RC deep beams and developed a concrete efficiency factor that captures the influence of web reinforcement. That work also evaluated the efficiency factors in ACI 318-19 and CSA and proposed a method to predict the concrete strength efficiency factor based on MCFT and concrete behavior.

1.1 Strut-and-Tie Formation

In STM, applied loads transfer to the supports through a network of compressive struts and tensile ties. Concrete struts (compressive fields) carry compression, while the longitudinal reinforcement resists tension. Nodes connect the struts and ties and maintain equilibrium between internal and external forces. Diagonal struts account for concrete softening in compression. Depending on the force path, struts may be prismatic, fan-shaped, or bottle-shaped, each reflecting a distinct force distribution within the beam (Kelareh et al., 2020) (Figure 1). STM simplifies the complex stress states that develop after cracking by representing stress flow as a truss. This approach clarifies behavior and enables more direct analysis in these regions. Beyond its analytical role, STM provides phenomenological insight into the behavior of structural concrete under load (Fan et al., 2022; Silveira et al., 2022; Karimizadeh and Arabzadeh., 2021). By adhering to the lower-bound theorem of plasticity, STM provides a conservative estimate of ultimate capacity, making it a dependable method for design and evaluation.

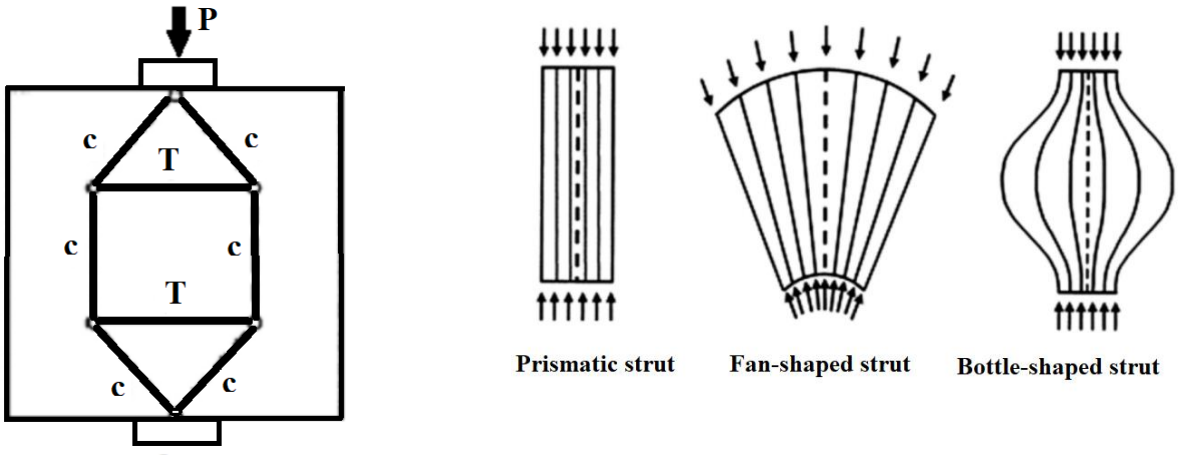

(a) (b)

Figure 1. (a) Strut-and-tie formation; (b) Types of struts (Kelareh et al., 2020)

1.2. Strut-and-Tie Model Approach for Deep Beams

Figure 2 shows a typical deep beam and its corresponding STM. The beam carries two vertical point loads on the top surface and is supported along the opposite face. The primary longitudinal reinforcement lies at a distance *d* from the top, and no web reinforcement is provided. If flexural strength is sufficient, failure is governed by compressive stresses within the strut, leading to diagonal crushing. STM predicts the shear strength carried by the diagonal struts, with shear following the strut path from load to support. In 2009, Arabzadeh et al. (2009) developed an STM-based model to predict the shear capacity of RC deep beams (Equation 1) and introduced an equation for the reduction coefficient of concrete strength. This model is used in the present study; further details appear in (Arabzadeh et al., 2009)

$$V_u = \frac{f_c^{\,0.7}}{0.7 + 0.15\left(\frac{a}{d}\right)^2} A_{str} \sin\theta + 0.065\rho_p^{-0.35} A_{wp} \cos\theta \quad (1)$$

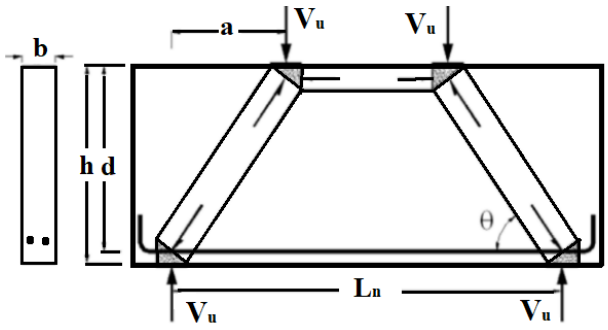

(a)

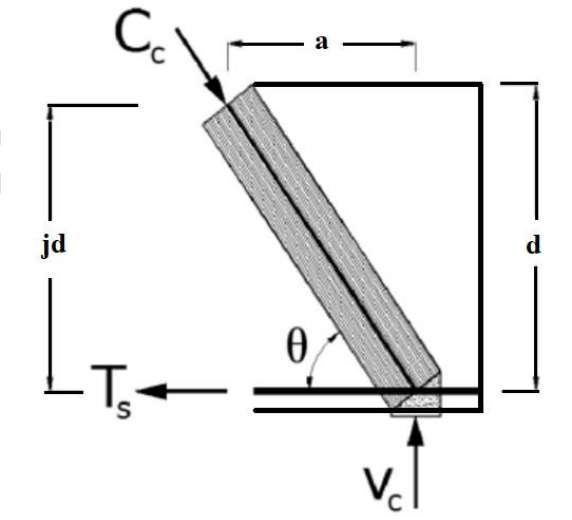

(b)

Figure 2. (a) Geometry of the concrete deep beam; (b) Equilibrium of the strut in the absence of web reinforcement (Arabzadeh et al.,2009)

1.3. Deep Beams under Dynamic Loads

Deep beams under dynamic loading exhibit more complex behavior than under static conditions (Yang et al. 2025; Petersona, 2025). Static loads apply gradually and remain constant, whereas dynamic loads are sudden and vary over time. In this study, dynamic loads refer to forces generated by vehicle movement on structural members. Prior work spans material testing to impact and blast analysis. Notably, Erzar and Forquin (2010) developed an experimental method to determine concrete tensile strength at high strain rates, and Grote et al. (2001) used Split Hopkinson Pressure Bar (SHPB) tests to characterize the dynamic behavior of concrete. These findings are implemented in commercial simulation software (e.g., LS-DYNA, ABAQUS) for nonlinear response under impact and blast loading. Under impact, the loading rate critically affects concrete behavior and must be considered for accurate results. Research shows that as strain rate increases, ultimate strength, elastic (secant) modulus, and peak strain also increase. By contrast, viscoelastic deformations such as creep occur under sustained loading, even at constant stress, and failure may occur at levels below quasi-static strength (Cusatis, 2011). Although this study focuses on vehicle-induced loads, understanding the behavior of members under other dynamic load types with different force-transfer mechanisms remains essential. For example, near-fault earthquakes can produce long-period velocity pulses that lead to deformation patterns and damage vulnerabilities distinct from high strain-rate impact loads (Ozturk, 2003). These differences support the need for analytical methods such as STM that can account for dynamic effects.

1.4. Dynamic Amplification Factor

This study introduces the dynamic amplification factor (D_I), defined as the ratio of shear capacity under dynamic two-point loading to shear capacity under static two-point loading. We use this ratio within the STM framework to develop a practical relationship for the concrete strength reduction factor in deep beams subjected to dynamic two-point loading. While STM is well established for static loading (Arabzadeh et al., 2009; ACI 318-19), its direct application to dynamic conditions remains limited. The literature on RC deep beams under dynamic loads is sparse, and many STM-based approaches for deep beams, as well as equations derived for slender beams, can over- or under-estimate capacity because of their empirical basis. Current codes and STM procedures rely on static properties and quasi-static analysis and provide no guidance for strain-rate–dependent enhancement of concrete strength. Although an empirical dynamic amplification factor (DAF) is sometimes used in bridge design for overall load effects, a mechanistic STM-based estimate of the concrete strength reduction factor (ν) at specified dynamic strain rates is absent. This study addresses that gap. The originality of this work lies in the development of a novel approximate equation, derived within the STM framework and incorporating an analytically-derived Dynamic Amplification Factor (D_I), to accurately predict the concrete strength reduction factor for reinforced concrete deep beams subjected to dynamic two-point concentrated loading across a range of strain rates. The approach integrates material-level dynamic effects directly into STM, providing a more rational and precise design procedure. Finite element analyses were conducted in ABAQUS. RC deep beams with three shear span-to-depth ratios were evaluated under four dynamic strain rates associated with vehicle effects, ranging from the minimum to the maximum values reported for such loading. Following Fujikake et al. (2000), the strength at the minimum rate (5.5×10^{-5}) is treated as quasi-static under vehicle effects, and the remaining three rates are

categorized as low, medium, and high (Table 1). Strengths obtained at these three rates are classified as dynamic.

Table 1. Dynamic Strain Rate Conditions.

Mode	Quasi Static	Low Dynamic	Medium Dynamic	High Dynamic
Strain Rate (ε) [1/s]	5.5×10^{-5}	1×10^{-4}	5.5×10^{-4}	1×10^{-3}

2. Research Significance

The structural behavior of deep beams under dynamic loading is more complex than under static conditions. A detailed examination of their behavior and failure mechanisms under dynamic loads, especially at ultimate states, is therefore essential. This study addresses this need by introducing the dynamic amplification factor (D_I). This factor provides a more accurate and practical basis for calculating the concrete strength reduction factor for deep beams under dynamic loading. Using the strut-and-tie model (STM), a consistent framework for assessing shear capacity under static loads, the study develops a new approximate equation to estimate the concrete strength reduction factor for deep beams subjected to dynamic two-point loading. The approach deepens understanding of deep-beam behavior under dynamic loads and provides a practical tool for improving the safety and efficiency of structures subjected to such actions.

2. Materials and Methods

2.1. Finite Element Modeling Framework

ABAQUS was used to develop finite element (FE) models of deep beams. Selecting an appropriate constitutive model is critical for simulating concrete under high-strain-rate dynamic loading, such as vehicular impact. The Karagozian & Case concrete (K&C) model was adopted for

this study. Its formulation includes a third, independent yield surface; removal of the tension cutoff and extension of plasticity in tension; a shifted pressure cutoff; a three-invariant description of the failure surfaces; a pressure-dependent triaxial extension-to-compression ratio; a shear-modulus correction; and a radial-path strain-rate enhancement (Malvar et al., 1997). The K&C model provides a physics-based representation of nonlinear concrete behavior suited to the objectives of this research. Additional details appear in Wu et al. (2011). Reinforcing bars were modeled with a uniaxial elastic–plastic material that incorporates strain-rate sensitivity and dependence on stress–strain history.

2.2. Element Types, Meshing, and Boundary Conditions

Concrete deep beams and the loading and bearing plates were modeled with three-dimensional eight-node, first-order, fully integrated continuum elements (C3D8). Reinforcing bars were modeled with three-dimensional two-node, first-order truss elements (T3D2). All elements used Gauss integration, and the nonlinear system was solved with the Newton-Raphson method. Boundary conditions in the tunnel formwork system were held constant throughout the analysis. The beams were modeled as simply supported, with constraints applied to reference points coupled to the support regions to simulate pin and roller conditions.

2.3. Assumptions and Limitations

The FE model adopted the following assumptions. It imposed a perfect bond between concrete and reinforcing steel, neglecting slip or local bond degradation under high-rate loading. Concrete followed the Karagozian & Case (K&C) constitutive model and was treated as a homogeneous, isotropic material with smeared cracking and strain-rate enhancement via a radial-path formulation (Malvar et al., 1997). The failure surfaces used a three-invariant formulation with simplified triaxial extension-to-compression ratios. The analyses captured strain-rate effects implicitly through the material model's dynamic definitions rather than explicit user-defined rate equations. A primary

limitation is reliance on calibrated parameters; however, validation against independent experimental data across loading rates and geometries mitigates this concern within the scope of the study.

2.4. Model Validation and Verification

The validation beam modeled in ABAQUS measured 150 × 250 × 1100 mm. The specimen was treated as a simply supported RC deep beam with supports at both ends and a dynamic point load applied at midspan (Figure 3). Concrete mechanical properties for the FE analysis followed the experimental program of Adikari et al. (2013). The modulus of elasticity for normal-weight concrete was calculated per ACI 318M as Ec = $4700\sqrt{f'c}$ MPa, and a Poisson's ratio of 0.20 was assumed for concrete in uniaxial compression. Concrete material properties and reinforcement specifications used in the model are provided in Table 2.

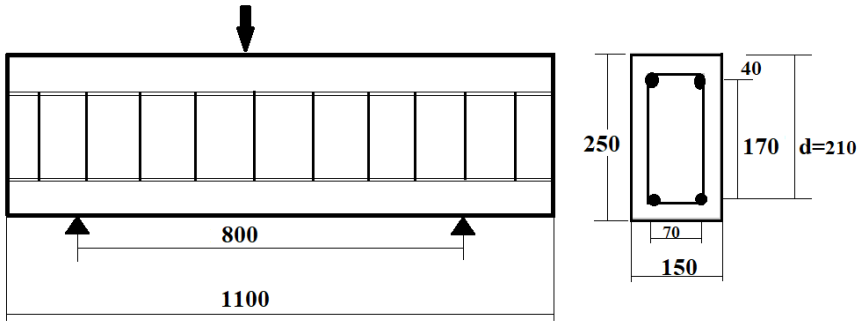

Figure 3. Dimensions of RC deep beams and layout of reinforcements in the Validation Process

Table 2. Characteristics of Concrete samples used in ABAQUS software

Sample	Upper reinforcement	Bottom reinforcement	Vertical shear reinforcement	$\acute{f}_c$(MPa)
Validated beam	2Φ22	2Φ22	10@100	40

To validate the FE modeling approach, a deep beam specimen previously tested experimentally

and analyzed in DIANA by Adhikary et al. (2013) was remodeled in ABAQUS. The predicted ultimate shear capacity, load–midspan deflection response, and failure modes were compared with both the experimental observations and the DIANA results. As shown in Table 3 and Figures 4–6, the ABAQUS simulations show close agreement with the benchmark data, confirming the accuracy and reliability of the modeling methodology under both static and dynamic loading.

Table 3. Comparison of Shear Resistance (kN)

Sample	Loading Rate (m/s)	Experimental	DIANA	ABAQUS (This study)
static	0.0004	271.9	300.2	295.3
Low rate	0.04	300.6	324	319.7
Medium rate	0.4	361.3	375.2	370.9
High rate	2	417	421.5	421

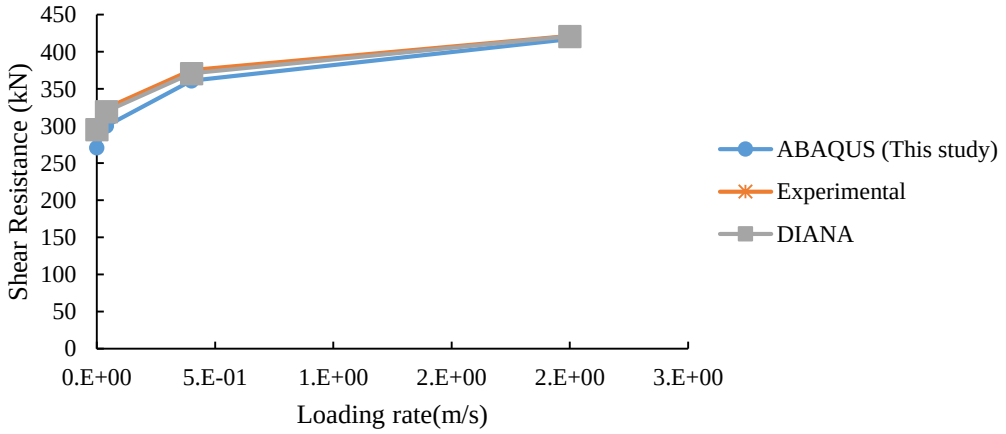

Figure 4. Validation of the numerical model against experimental and DIANA simulation results for dynamic shear resistance under various loading rates.

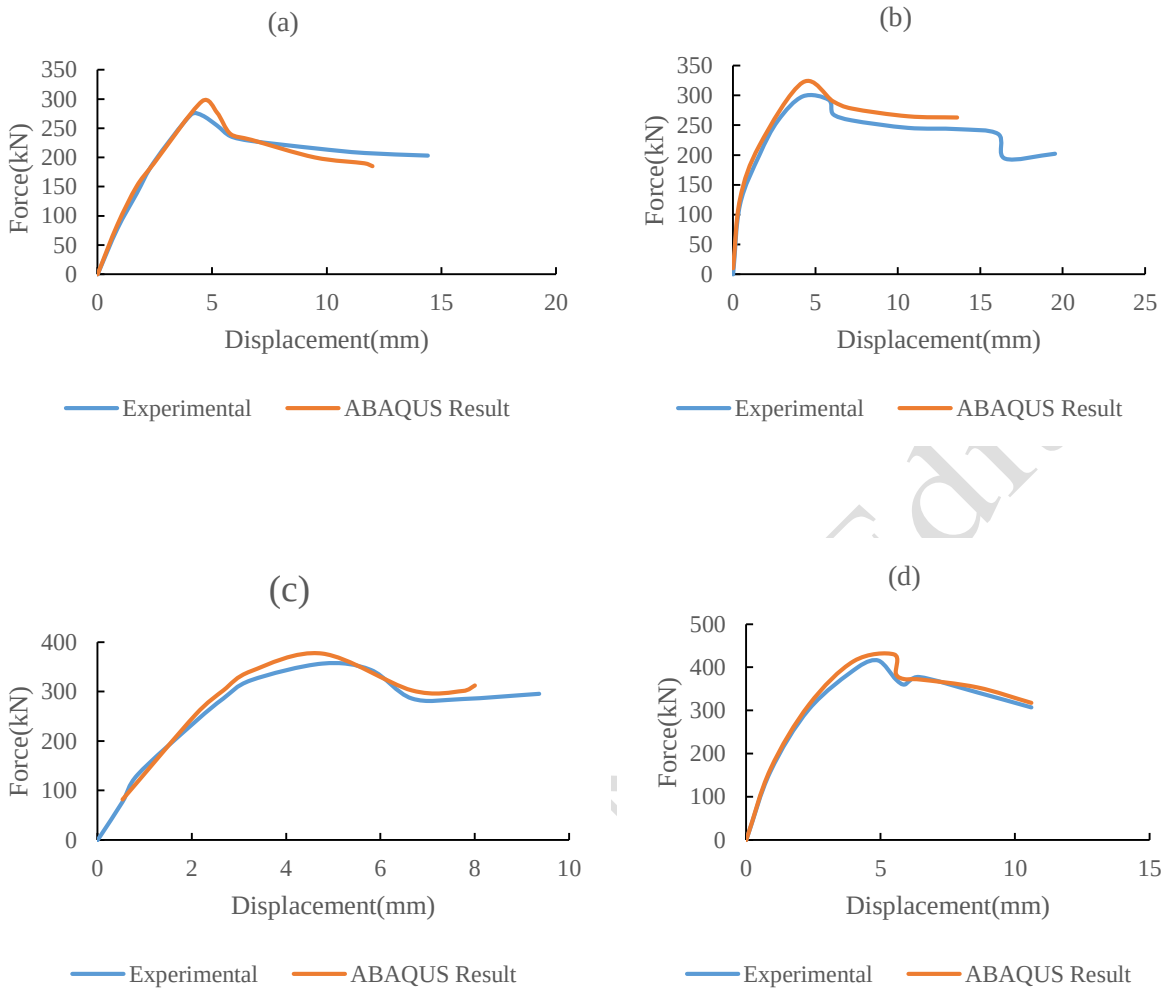

Figure 5. Validation of the finite element model: Comparison of experimental and simulated load–midspan deflection curves for the specimen under (a) static, (b) low, (c) medium, and (d) high loading rates.

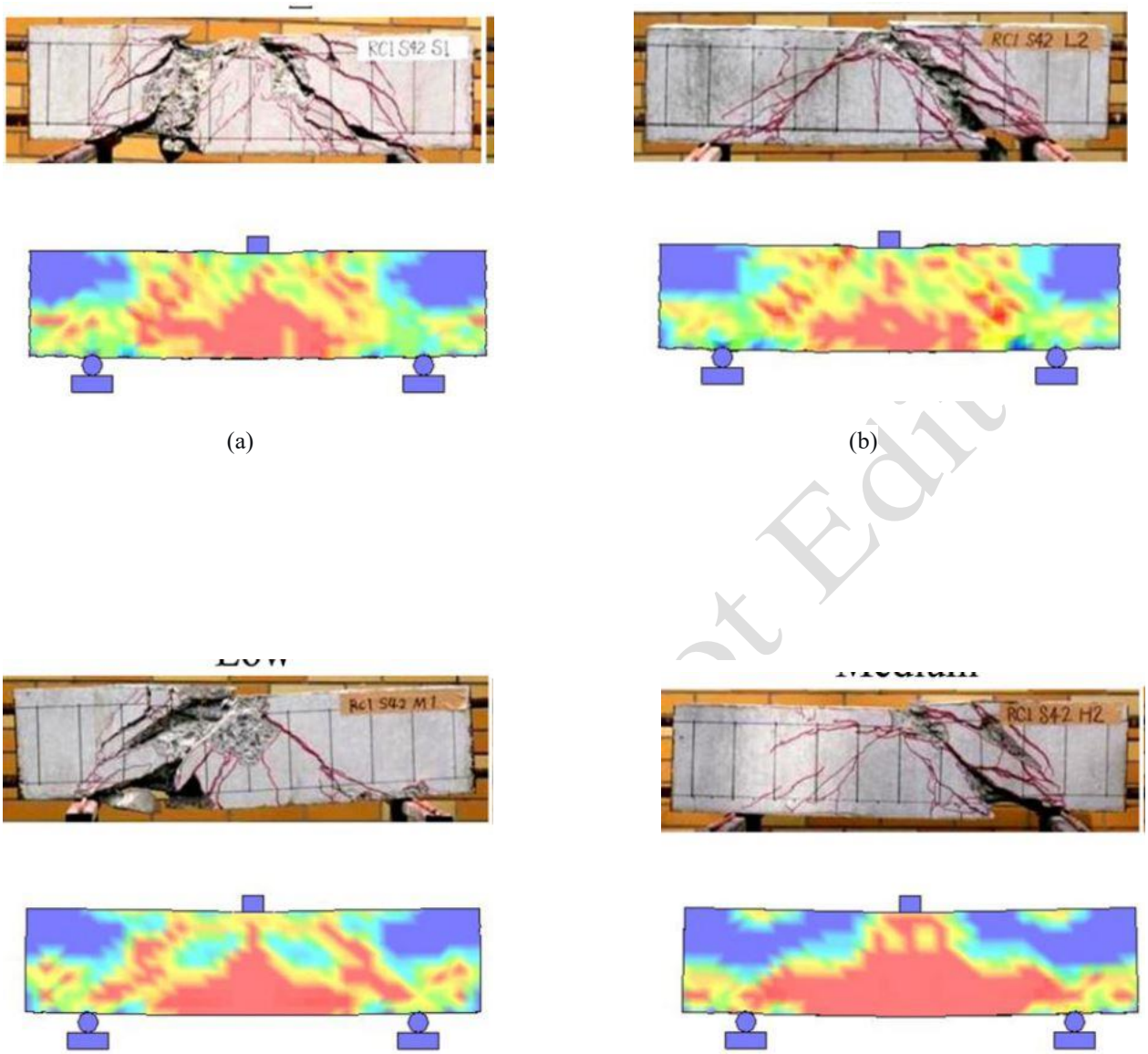

Figure 6. Comparison of failure mode under(a) static loading, (b) low dynamic loading, medium dynamic loading, and high dynamic loading.

3. Analytical Approach

After validating the finite element (FE) modeling approach, a parametric study was conducted to meet the core objectives of the research. Two categories of reinforced concrete (RC) deep beams were analyzed: 2000 × 900 × 140 mm and 2000 × 450 × 140 mm. All beams carried two-point

loads on the top surface. For each category, three shear span-to-depth ratios (a/d) were examined to evaluate their influence on behavior. The study varied concrete compressive strength (f'c), the span length-to-depth ratio (l/h), the shear span-to-depth ratio (a/d), and the strain rate ($\dot{\varepsilon}$) to assess their effects on the shear strength of the deep beams. The structural response was obtained with pushover analysis in ABAQUS, incrementally increasing load to ultimate capacity to determine the peak load and corresponding displacement. The analysis employed FE modeling within the strut-and-tie model (STM) framework to investigate behavior under static and dynamic two-point loading. The dynamic analysis considered strain rates associated with vehicle effects, from quasi-static to high-rate. Numerical results were then compared with shear capacities from a simplified STM-based formulation for static loading previously developed by the author. Using this comparison and the analytically derived dynamic amplification factor (D_I) (the ratio of dynamic to static shear capacity), a new approximate equation was formulated to predict the concrete strength reduction factor for deep beams under dynamic two-point loading. The equation showed approximately 99% accuracy and provides a reliable basis for designing deep beams subjected to dynamic loads. Detailed model specifications appear in the tables and figures below.

Table 4. Details of the Analytical Models

Series	Total Length (mm)	Clear Length (lc) (mm)	h (mm)	b (mm)	d (mm)	Transverse Reinforcement (Diameter and Spacing)	Longitudinal Reinforcement (Diameter)	Yield Strength of Longitudinal Reinforcement (MPa)	Yield Strength of transverse Reinforcement (MPa)
1	2000	1800	900	140	800	1Φ10@10cm	2 Φ 22	371	342
2	2000	1800	450	140	400	1Φ10@10cm	2 Φ 22	371	342

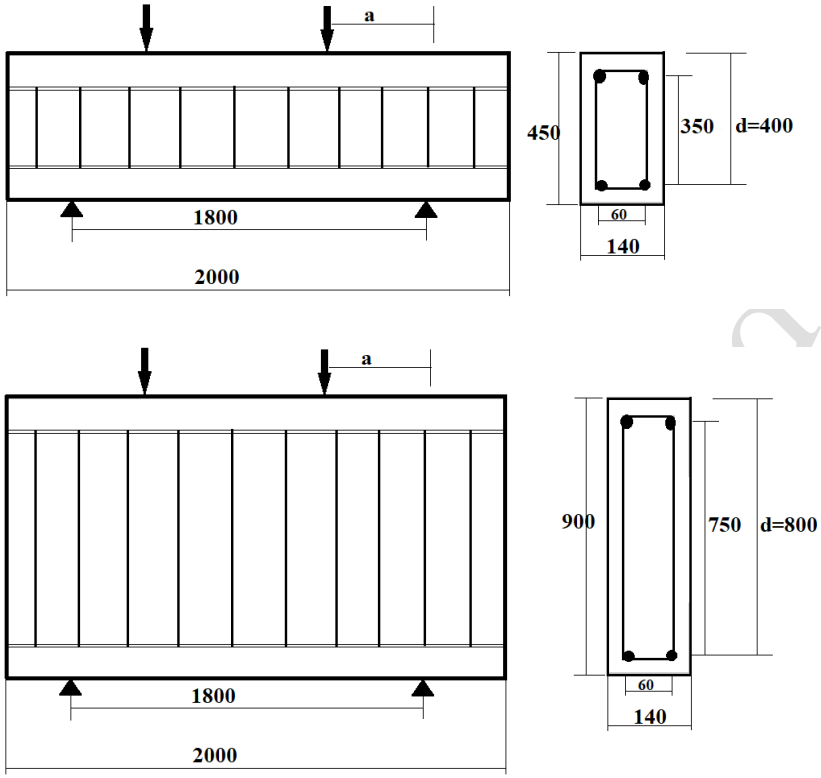

Figure 7. Details of Samples

4. Discussion and Results Analysis

The analytical results of all the specimens are presented in the following Tables.

Table 5. The analytical results of specimens with fc=25 MPa

F_c MPa	L	L/h	h	d	a/d	a	shear (kN)			
							5.50E-05	1.00E-04	5.50E-04	1.00E-03
25	1.8	2	0.9	0.8	0.35	0.28	277.77	301.59	298.09	313.44
					0.7	0.56	269.50	292.08	287.06	295.97
					1.1	0.88	259.53	285.20	281.93	274.00
		4	0.45	0.4	0.7	0.28	173.19	181.74	179.25	181.84
					1.4	0.56	161.41	172.28	170.01	168.45
					2.1	0.85	149.77	161.48	155.82	159.81

Table 6. The analytical results of specimens with fc=30 MPa

F_c MPa	L	L/h	h	d	a/d	a	shear (kN)			
							5.50E-05	1.00E-04	5.50E-04	1.00E-03
30	1.8	2	0.9	0.8	0.35	0.28	310.10	336.79	343.14	368.27
					0.7	0.56	303.38	326.69	330.93	348.10
					1.1	0.88	290.83	319.67	325.67	322.51
		4	0.45	0.4	0.7	0.28	190.12	199.64	203.09	210.38
					1.4	0.56	177.45	189.62	193.04	195.07
					2.1	0.85	165.01	178.08	177.11	185.49

Table 7. The analytical results of specimens with fc =40 MPa

F_c MPa	L	L/h	h	d	a/d	a	shear (kN)			
							5.50E-05	1.00E-04	5.50E-04	1.00E-03
40	1.8	2	0.9	0.8	0.35	0.28	346.2	376.1	395	432.7
					0.7	0.56	339.4	365.4	381.5	409.4
					1.1	0.88	325.9	358.3	376.2	379.6
		4	0.45	0.4	0.7	0.28	208.7	219.3	230.1	243.4
					1.4	0.56	195.1	208.7	219.2	225.9
					2.1	0.85	181.8	196.4	201.3	215.3

Table 8. The analytical results of specimens with fc =50 MPa

F_c MPa	L	L/h	h	d	a/d	a	shear (kN)			
							5.50E-05	1.00E-04	5.50E-04	1.00E-03
50	1.8	2	0.9	0.8	0.35	0.28	386.5	420.0	454.7	508.4
					0.7	0.56	379.7	408.7	439.8	481.5
					1.1	0.88	365.2	401.6	434.6	446.8
		4	0.45	0.4	0.7	0.28	229.1	240.9	260.7	281.6
					1.4	0.56	214.5	229.7	248.9	261.6
					2.1	0.85	200.3	216.6	228.8	249.9

4.1. Shear Resistance and Strain Rate

An analysis of Tables 5–8 shows that strain rate significantly affects the shear strength of RC deep beams. Quantitatively, shear resistance at the maximum strain rate is about 18.5% higher than at the minimum rate. This increase reflects the rate-dependent behavior of the constituent materials.

At higher loading rates, concrete develops fewer microcracks because less time is available for energy dissipation through crack growth, which increases the apparent stiffness and strength as the member absorbs energy through higher-capacity mechanisms. As a result, the initiation and propagation of shear and flexural cracks are delayed, the failure mode shifts, and the overall shear capacity rises. These results are consistent with the known rate-dependent response of quasi-brittle materials under dynamic loading (Bischoff and Perry.,1991; Malvar et al.,1997).

4.2. Effects of Shear Span-to-Depth Ratio (a/d) on the Shear Strength of Deep Beams

The shear span-to-depth ratio (a/d) governs the shear behavior of deep beams because it influences the formation and propagation of tensile cracks near supports and loading points and thus the ultimate shear capacity. The results show a consistent trend: increasing a/d reduces shear strength across all strain rates and for both beam categories. This inverse relationship reflects a transition in failure mechanism. At lower a/d, failure is dominated by strut crushing, which engages a larger concrete compression zone and yields higher capacity. As a/d increases, the mode shifts to a flexure–shear interactive failure with critical diagonal cracking and yielding of transverse reinforcement, which has lower load-carrying capacity. Prior studies under static loading report the same trend (Zhang and Tan., 2007; ACI Committee 318., 2019). The present study confirms that this relationship holds under high-rate dynamic loading. Although rate effects raise the absolute shear strength at all a/d ratios, they do not change the fundamental inverse correlation between a/d and shear capacity.

4.3. Effects of the Span Length-to-Depth Ratio (L/H) on Shear Strength

The tabulated results show that the shear strength of RC deep beams decreases as the span-to-depth ratio (l/h) increases. This reduction reflects a shift in structural behavior: as l/h grows, the response transitions from a shear-dominated deep beam, where arching action governs, to a

bending-dominated slender beam, where beam action prevails (Zhang and Tan, 2007). In deep beams with low l/h, load transfers to the supports primarily through a direct compressive strut, which produces higher shear capacity. At higher l/h, bending moments become more influential, flexural cracks develop, and the contribution of the arching mechanism declines, reducing overall shear strength. This well-documented transition, which supports the accuracy of the present FE model, has been reported under static loading [Appa Rao and Kunal., 2007]. The current results show that the same relationship holds under dynamic loading, with rate effects increasing shear capacity across all l/h values without changing the underlying trend.

4.4. Validation Against a Strut-and-Tie Model and Comparative Analysis

The shear strength under static loading was computed with the simplified strut-and-tie model (STM) proposed by Arabzadeh et al. (2009) (Eq. 1) for both beam categories, providing a baseline for evaluating the dynamic response. STM predictions were then compared with shear strengths from the finite element method (FEM) at the minimum dynamic strain rate. As shown in Tables 9–12 and Figure 8, STM values are, on average, 5% lower than FEM results, indicating that the simplified STM gives conservative estimates of shear capacity, which is advantageous for design. The difference likely reflects STM simplifications that do not fully capture stress redistribution and confinement effects represented in nonlinear FEM. The comparison also shows consistent geometric sensitivity in both methods: increasing the shear span-to-depth ratio (a/d) reduces shear strength in both STM and FEM, as illustrated in Figure 8.

Table 9. Comparison of Shear Strengths: Strut-and-Tie Model and Finite Element Method (Static, Minimum Strain Rate) for specimens with fc=25 MPa

Fc	L/h	h	d	a/d	a	shear (kN)		
						STM	FEM	$\frac{V_{STM}}{V_{FEM}}$
25	2	0.9	0.8	0.35	0.28	252.6	277.8	0.91
				0.7	0.56	249.2	269.5	0.92
				1.1	0.88	247.1	259.5	0.95
	4	0.45	0.4	0.7	0.28	153.4	173.2	0.89
				1.4	0.56	149.3	161.4	0.93
				2.1	0.85	142.1	149.8	0.95

Table 10. Comparison of Shear Strengths: Strut-and-Tie Model and Finite Element Method (Static, Minimum Strain Rate) for specimens with fc=30 MPa

Fc	L/h	h	d	a/d	a	shear (kN)		
						STM	FEM	$\frac{V_{STM}}{V_{FEM}}$
30	2	0.9	0.8	0.35	0.28	279.5	310.1	0.90
				0.7	0.56	279.3	303.4	0.92
				1.1	0.88	274.3	290.8	0.94
	4	0.45	0.4	0.7	0.28	170.6	190.1	0.90
				1.4	0.56	164.2	177.5	0.93
				2.1	0.85	154.4	165.0	0.94

Table 11. Comparison of Shear Strengths: Strut-and-Tie Model and Finite Element Method (Static, Minimum Strain Rate) for specimens with fc =40 MPa

Fc	L/h	h	d	a/d	a	shear (kN)		
						STM	FEM	$\frac{V_{STM}}{V_{FEM}}$
40	2	0.9	0.8	0.35	0.28	331.6	346.2	0.96
				0.7	0.56	328.1	339.4	0.97
				1.1	0.88	319.4	325.9	0.98
	4	0.45	0.4	0.7	0.28	189.6	208.7	0.91
				1.4	0.56	180.5	195.1	0.93
				2.1	0.85	171.4	181.8	0.94

Table 12. Comparison of Shear Strengths: Strut-and-Tie Model and Finite Element Method (Static, Minimum Strain Rate) for specimens with fc =50 MPa

Fc	L/h	h	d	a/d	a	shear (kN)		
						STM	FEM	$\frac{V_{STM}}{V_{FEM}}$
50	2	0.9	0.8	0.35	0.28	367.2	386.5	0.95
				0.7	0.56	362.6	379.7	0.96
				1.1	0.88	352.6	365.2	0.97
	4	0.45	0.4	0.7	0.28	210.8	229.1	0.92
				1.4	0.56	198.4	214.5	0.93
				2.1	0.85	190.3	200.3	0.95

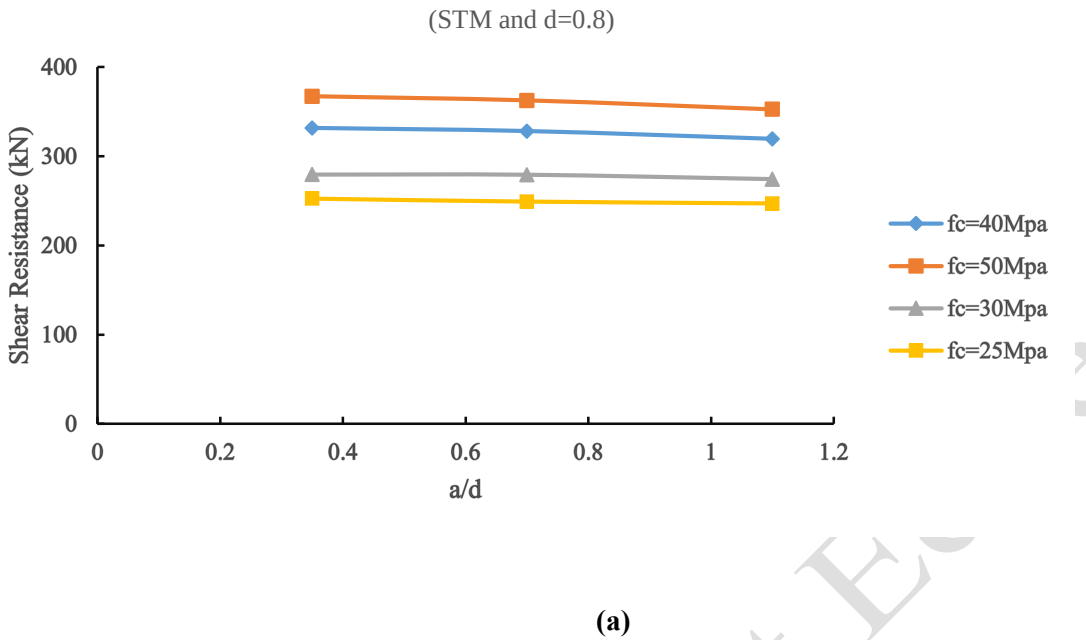

(a)

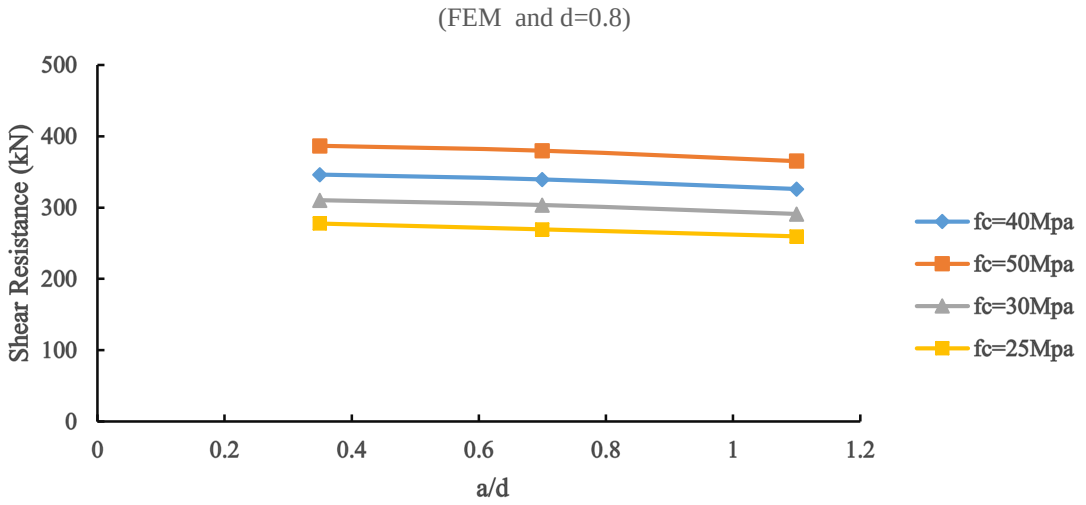

(b)

Figure 8. Effect of the shear span-to-depth ratio (a/d) on the shear strength of reinforced concrete deep beams in (a)STM and (b) FEM analyses

4.5. Dynamic Amplification Factor (D_1)

The dynamic amplification factor (D_1) quantifies the increase in shear capacity under dynamic loading relative to the static baseline. Tables 13–16 list D_1 values from the finite element analysis and show its dependence on geometric ratios (a/d, L/h), concrete compressive strength (f_c), and the loading rate itself. A consistent trend appears: D_1 decreases as the span-to-depth ratio (L/h) increases (Fig. 9). This reflects a shift in governing behavior. At low L/h, true deep-beam action prevails and arching governs shear resistance; this efficient mechanism shows stronger positive rate effects. As L/h increases, the response shifts toward beam action, which is more flexure-dominated and less rate sensitive, so the amplification factor declines. The interaction between a/d and strain rate further clarifies the response. For beams with L/h = 2 (Fig. 10(a)), the amplification trend reverses at the highest rate, suggesting a change in the failure mode's rate sensitivity. At lower a/d ratios, failure is predominantly shear controlled (for example, diagonal splitting) and highly rate sensitive. At higher a/d ratios, the mode shifts toward flexure–shear interaction, which exhibits a weaker dynamic enhancement, producing the observed reduction in D_1 t the highest rate. Material strength also matters. Plotting D_1 against normalized compressive strength (fc/20) (Fig. 11) shows that higher-strength concretes exhibit larger increases in D_1 at moderate and high strain rates, likely due to denser microstructure, greater brittleness, and correspondingly higher fracture energy with altered cracking patterns. At slow rates, this influence is negligible.

Table 13. Shear resistance values and Dynamic Amplification Factor (D_1) for beams with a concrete compressive strength of 25 MPa.

F_c	L/h	h	d	a/d	a	shear (kN)				$D_1 = \frac{V_{dyn}}{V_{sta}}$		
						5.50E-05	1.00E-04	5.50E-04	1.00E-03	1.00E-04	5.50E-04	1.00E-03
25	2	0.9	0.8	0.35	0.28	277.77	301.59	298.09	313.44	1.09	1.07	1.13
				0.7	0.56	269.50	292.08	287.06	295.97	1.08	1.07	1.10
				1.1	0.88	259.53	285.20	281.93	274.00	1.10	1.09	1.06
	4	0.45	0.4	0.7	0.28	173.19	181.74	179.25	181.84	1.05	1.04	1.05
				1.4	0.56	161.41	172.28	170.01	168.45	1.07	1.05	1.04
				2.1	0.85	149.77	161.48	155.82	159.81	1.08	1.04	1.07

Table 14. Shear resistance values and Dynamic Amplification Factor (D_1) for beams with a concrete compressive strength of 30 MPa.

F_c	L/h	h	d	a/d	a	shear (kN)				$D_1 = \frac{V_{dyn}}{V_{sta}}$		
						5.50E-05	1.00E-04	5.50E-04	1.00E-03	1.00E-04	5.50E-04	1.00E-03
30	2	0.9	0.8	0.35	0.28	310.10	336.79	343.14	368.27	1.09	1.11	1.19
				0.7	0.56	303.38	326.69	330.93	348.10	1.08	1.09	1.15
				1.1	0.88	290.83	319.67	325.67	322.51	1.10	1.12	1.11
	4	0.45	0.4	0.7	0.28	190.12	199.64	203.09	210.38	1.05	1.07	1.11
				1.4	0.56	177.45	189.62	193.04	195.07	1.07	1.09	1.10
				2.1	0.85	165.01	178.08	177.11	185.49	1.08	1.07	1.12

Table 15. Shear resistance values and Dynamic Amplification Factor (D_1) for beams with a concrete compressive strength of 40 MPa.

F_c	L/h	h	d	a/d	a	shear (kN)				$D_1 = \frac{V_{dyn}}{V_{sta}}$		
						5.50E-05	1.00E-04	5.50E-04	1.00E-03	1.00E-04	5.50E-04	1.00E-03
40	2	0.9	0.8	0.35	0.28	346.2	376.1	395	432.7	1.09	1.14	1.25
				0.7	0.56	339.4	365.4	381.5	409.4	1.08	1.12	1.21
				1.1	0.88	325.9	358.3	376.2	379.6	1.10	1.15	1.16
	4	0.45	0.4	0.7	0.28	208.7	219.3	230.1	243.4	1.05	1.10	1.17
				1.4	0.56	195.1	208.7	219.2	225.9	1.07	1.12	1.16
				2.1	0.85	181.8	196.4	201.3	215.3	1.08	1.11	1.18

Table 16. Shear resistance values and Dynamic Amplification Factor (D_1) for beams with a concrete compressive strength of 50 MPa.

F_c	L/h	h	d	a/d	a	shear (kN)				$D_1 = \frac{V_{dyn}}{V_{sta}}$		
						5.50E-05	1.00E-04	5.50E-04	1.00E-03	1.00E-04	5.50E-04	1.00E-03
50	2	0.9	0.8	0.35	0.28	386.5	420.0	454.7	508.4	1.09	1.18	1.32
				0.7	0.56	379.7	408.7	439.8	481.5	1.08	1.16	1.27
				1.1	0.88	365.2	401.6	434.6	446.8	1.10	1.19	1.22
	4	0.45	0.4	0.7	0.28	229.1	240.9	260.7	281.6	1.05	1.14	1.23
				1.4	0.56	214.5	229.7	248.9	261.6	1.07	1.16	1.22
				2.1	0.85	200.3	216.6	228.8	249.9	1.08	1.14	1.25

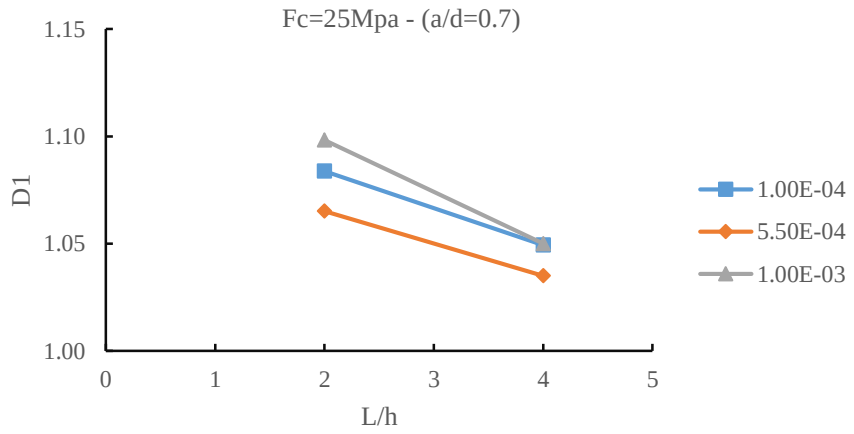

(a)

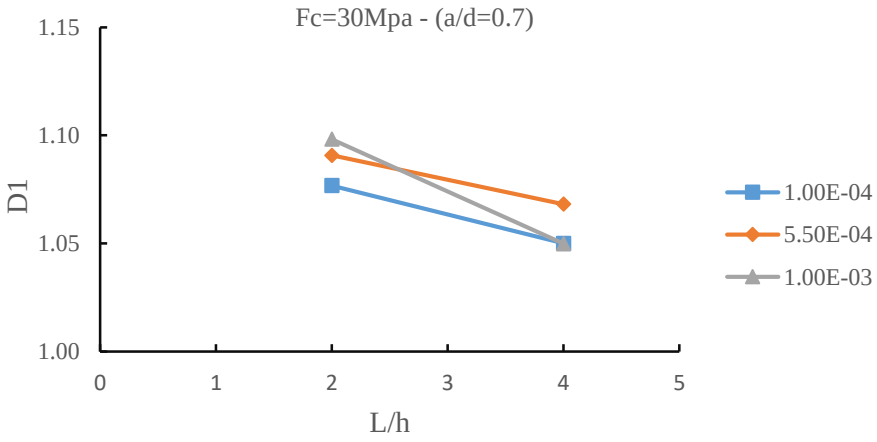

(b)

Figure 9. The variation of D_1 concerning the span length-to-depth ratio (L/h) for deep beams under different material properties and dynamic loading conditions (a) f_c=25 MPa; (b) f_c=30 MPa

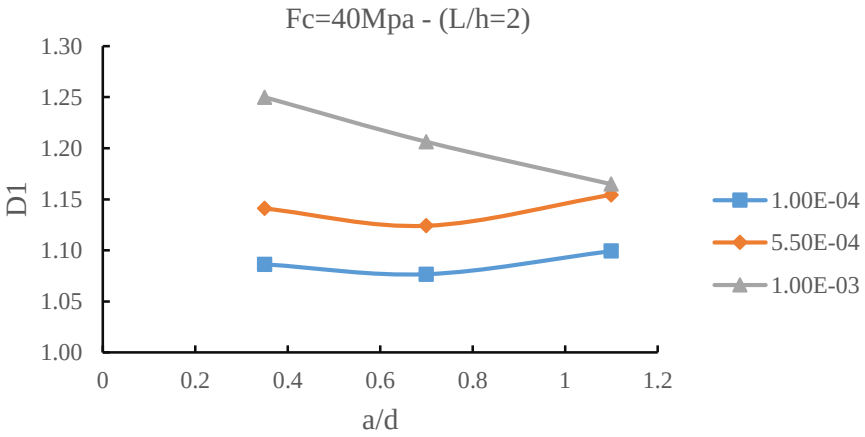

(a)

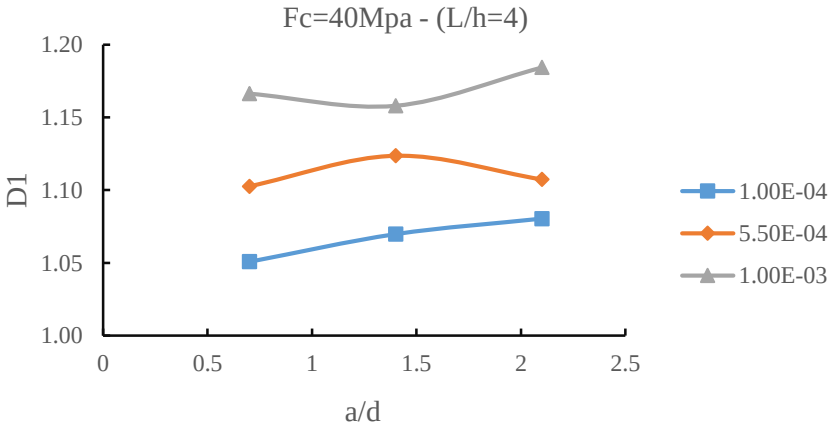

(b)

Figure 10. The variation of D_1 to shear span-to-depth ratio (a/d) for deep beams under different dynamic loading conditions (a) with L/h = 2; (b) with L/h = 4

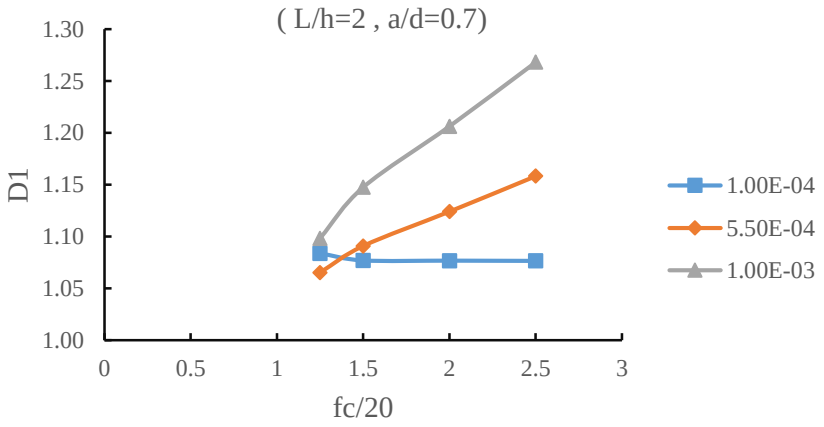

(a)

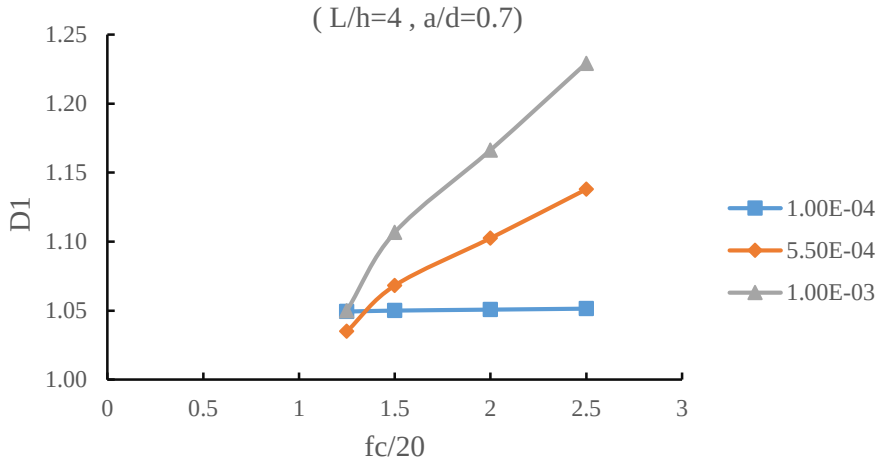

(b)

Figure11. Dynamic Amplification Factor (D_1)- dimensionless parameter (fc/20) curve, for deep beams under different dynamic loading conditions(a) with L/h = 2; (b) with L/h = 4

5. Sensitivity Analysis

A rigorous sensitivity and uncertainty analysis was performed to evaluate the robustness of the numerical models and the subsequent empirical equation proposed for calculating the concrete strength reduction factor in deep reinforced concrete beams subjected to dynamic two-point concentrated loading (ν_{dyn}). This process is essential for verifying the reliability of the findings

and for assessing their potential variability under different conditions. The sensitivity of the key output, the Dynamic Amplification Factor (D_I) and by extension ν_{dyn}, to variations in the primary input parameters was thoroughly investigated. These parameters include the concrete compressive strength (fc), the span-to-depth ratio (L/h), the shear span-to-depth ratio (a/d), and the strain rate ($\dot{\varepsilon}$). The analysis of the comprehensive results presented in Tables 13-16 and Figures 9-11 reveals a distinct hierarchy in parameter sensitivity:

Strain Rate ($\dot{\varepsilon}$): This parameter demonstrated the most significant influence on the dynamic response. For example, increasing the strain rate from the quasi-static level to the high dynamic level, led to an increase in D_I of up to 32% for beams with $\frac{L}{h} = 2$ and $f_c = 50MPa$ (Table 16). The sensitivity to strain rate is markedly higher in high-strength concrete and in beams with lower L/h ratios, where arching action dominates.

Concrete Compressive Strength (fc**):** The model shows considerable sensitivity to the concrete strength, particularly under medium to high strain rates. The dynamic enhancement is more pronounced for higher-strength concretes, as evidenced by the increasing slope of the D_I versus fc/20 curves in Figure 11. This is attributed to the more brittle nature and denser microstructure of high-strength concrete, which responds more significantly to rapid loading.

Geometric Ratios (a/d **and** L/h**):** The influence of geometric parameters is complex and exhibits a strong interaction with the loading rate. The a/d ratio has a moderate to high influence, whose effect can even reverse (from positive to negative correlation with D_I) at very high strain rates for specific configurations, such as those with $\frac{L}{h} = 2$ (Figure 10a). This suggests a shift in the failure mode's sensitivity. Conversely, the L/h ratio consistently shows a negative correlation with D_I, indicating that beams exhibiting more flexure-dominated behavior (higher L/h) are less sensitive to dynamic effects than those failing in shear (lower L/h).This established sensitivity hierarchy

(ε̇>fc>Geometric Ratios) confirms that the model's predictions are most strongly governed by the loading rate and material properties, which is consistent with the fundamental physics of rate-dependent material behavior.

6. Introduction of a New Approximate Formula for the Concrete Strength Reduction Factor in Deep Reinforced Concrete Beams under Dynamic Two-Point Concentrated Loading Using the Truss Model

This section presents an approximate equation for the concrete strength reduction factor in deep reinforced concrete beams subjected to dynamic two-point loading. The relationship builds on the author's earlier strut-and-tie model (STM) method for static two-point loading (Eq. 1) and extends that framework to dynamic conditions. Across the analyzed cases, the proposed equation achieved about 99% accuracy.

$$V_u = \frac{{f_c}^{0.7}}{0.7 + 0.15\left(\frac{a}{d}\right)^2} A_{str} \sin\theta + 0.065\rho_p^{-0.35} A_{wp} \cos\theta \quad (1)$$

$$\frac{V_{u_{stm_{dyn}}}}{V_{u_{stm_{static}}}} = \frac{V_{u_{F.N_{dyn}}}}{V_{u_{F.N_{static}}}} = D_1 (2)$$

In Equation (1,2), the concrete strength reduction factor under static loading conditions is expressed as follows:

$$\nu_{static} f_c = \frac{f_c^{0.7}}{0.7 + 0.15\left(\frac{a}{d}\right)^2} (3)$$

$$\nu_{static} = \frac{f_c^{-0.3}}{0.7 + 0.15\left(\frac{a}{d}\right)^2} (4)$$

The calculated values of the concrete strength reduction factor under static loading conditions for all the investigated beams in this study are presented in the following table.

Table 17. The calculated values of the concrete strength reduction factor under static loading conditions for beams with a concrete compressive strength of 25MPa

$\frac{f_c'}{20}$	L/h	h	d	a/d	a	ν	$d_1 = \frac{\nu_{dyn}}{\nu_{sta}}$		
						static	$\frac{\dot{o}}{5.50E-05} = 1.82$	$\frac{\dot{o}}{5.50E-05} = 10$	$\frac{\dot{o}}{5.50E-05} = 18.18$
1.25	2	0.9	0.8	0.35	0.28	0.53	1.32	1.30	1.36
	2	0.9	0.8	0.7	0.56	0.49	1.41	1.37	1.41
	2	0.9	0.8	1.1	0.88	0.43	1.84	1.81	1.77
	4	0.45	0.4	0.7	0.28	0.49	1.98	1.94	1.98
	4	0.45	0.4	1.4	0.56	0.38	3.39	3.34	3.32
	4	0.45	0.4	2.1	0.85	0.28	6.11	5.89	6.04

Table 18. The calculated values of the concrete strength reduction factor under static loading conditions for beams with a concrete compressive strength of 30 MPa

$\frac{f_c'}{20}$	L/h	h	d	a/d	a	ν	$d_1 = \frac{\nu_{dyn}}{\nu_{sta}}$		
						static	$\frac{\dot{o}}{5.50E-05} = 1.82$	$\frac{\dot{o}}{5.50E-05} = 10$	$\frac{\dot{o}}{5.50E-05} = 18.18$
1.5	2	0.9	0.8	0.35	0.28	0.50	1.30	1.32	1.42
	2	0.9	0.8	0.7	0.56	0.47	1.36	1.38	1.45
	2	0.9	0.8	1.1	0.88	0.41	1.80	1.83	1.83

	4	0.45	0.4	0.7	0.28	0.47	1.87	1.91	1.98
	4	0.45	0.4	1.4	0.56	0.36	3.28	3.33	3.36
	4	0.45	0.4	2.1	0.85	0.26	6.04	6.00	6.27

Table 19. The calculated values of the concrete strength reduction factor under static loading conditions for beams with a concrete compressive strength of 40 MPa

$\frac{f_c'}{20}$	**L/h**	**h**	**d**	**a/d**	**a**	ν	$d_1 = \frac{\nu_{dyn}}{\nu_{sta}}$		
						static	$\frac{\dot{\varepsilon}}{5.50E-05} = 1.82$	$\frac{\dot{\varepsilon}}{5.50E-05} = 10$	$\frac{\dot{\varepsilon}}{5.50E-05} = 18.18$
2	2	0.9	0.8	0.35	0.28	0.46	1.17	1.24	1.37
	2	0.9	0.8	0.7	0.56	0.43	1.26	1.30	1.40
	2	0.9	0.8	1.1	0.88	0.38	1.63	1.71	1.74
	4	0.45	0.4	0.7	0.28	0.43	1.70	1.77	1.88
	4	0.45	0.4	1.4	0.56	0.33	2.94	3.09	3.18
	4	0.45	0.4	2.1	0.85	0.24	5.38	5.50	5.88

Table 20. The calculated values of the concrete strength reduction factor under static loading conditions for beams with a concrete compressive strength of 50 MPa

$\frac{f_c'}{20}$	**L/h**	**h**	**d**	**a/d**	**a**	ν	$d_1 = \frac{\nu_{dyn}}{\nu_{sta}}$		
						static	$\frac{\dot{\varepsilon}}{5.50E-05} = 1.82$	$\frac{\dot{\varepsilon}}{5.50E-05} = 10$	$\frac{\dot{\varepsilon}}{5.50E-05} = 18.18$
2.5	2	0.9	0.8	0.35	0.28	0.43	1.14	1.23	1.37
	2	0.9	0.8	0.7	0.56	0.40	1.20	1.28	1.40
	2	0.9	0.8	1.1	0.88	0.35	1.57	1.71	1.77
	4	0.45	0.4	0.7	0.28	0.40	1.60	1.73	1.88
	4	0.45	0.4	1.4	0.56	0.31	2.74	2.97	3.10
	4	0.45	0.4	2.1	0.85	0.23	4.91	5.17	5.65

It is important to note that the two independent variables, fc and ε̇, are normalized as fc/20 and ε̇/(5.5×10−5), respectively, to render them dimensionless.

The following relationship is derived for calculating the concrete strength reduction factor under various dynamic two-point concentrated loading conditions:

$$\frac{\nu_{dyn}}{\nu_{static}} = d_1 (5)$$

Based on the derived relationship and the values presented in the tables above, a correlation between the independent variables fc, L/h, a/d, and ε̇, and the dependent variable ν_{dyn} is established through regression analysis.

$$\nu_{dyn} = d_1 . \nu_{static} (6)$$

$$d_1 = 1.874 - 0.225\left(\frac{f_c}{20}\right) + 0.013e^{\frac{L}{h}} - 1.46\left(\frac{a}{d}\right) + 1.503\left(\frac{a}{d}\right)^2 + 0.01\left(\frac{\dot{\varepsilon}}{5.5\times10^{-5}}\right) (7)$$

7. Uncertainty Analysis Based on Regression Statistics

The uncertainty in the predictions of the proposed empirical equation (Eq. 6) was quantified using the statistics derived from the multivariate regression analysis. The primary sources of uncertainty include the inherent variability in material properties and the approximations inherent in the finite element modeling process. SPSS output indicates a very strong correlation between the independent variables and the dependent variable D_1 (R-value of 0.996). The coefficient of determination (R^2 = 0.991) shows that the model explains about 99.1% of the variance in D_1, demonstrating high predictive power. The standard error of 0.15312 indicates precise predictions. These results confirm that the proposed regression model reliably predicts D_1 and can be used in future studies.

8. Conclusions

his study numerically examined the dynamic shear response of reinforced concrete deep beams across a wide range of loading rates, geometric configurations, and material strengths. The main conclusions are as follows. The finite element model in ABAQUS reliably simulated the rate-dependent shear behavior of deep beams, as verified against experimental benchmarks and by comparison with DIANA and an analytical strut-and-tie model (STM). The dynamic amplification factor (D_1) for shear capacity is not constant; it depends on loading rate, shear span-to-depth ratio (a/d), span-to-depth ratio (L/h), and concrete compressive strength (f_c). The influence of geometric parameters (a/d, L/h) on shear strength, well established under static loading, persists under dynamic conditions, with rate effects increasing capacity across all configurations.

A new empirical equation was developed to predict the dynamic concrete strength reduction factor (ν_dyn). The model, derived from multivariate regression ($R^2 = 0.991$), captures the interaction among all investigated parameters and offers practical advantages. Its primary significance lies in providing designers with a robust, computationally efficient STM-based tool for assessing dynamic shear capacity without resorting to full nonlinear finite element analysis. This work helps bridge the gap between simplified static methods and sophisticated dynamic simulations. Future research should experimentally validate these findings at high loading rates and extend the model to a broader parameter space and loading scenarios, including impact and blast.

Acknowledgments

The authors would like to sincerely thank the Department of Civil Engineering at Razi University of Kermanshah for their scientific support, as well as the valuable guidance of the supervising and

advising professors during the course of this research. This study was conducted without any direct financial support.

9.References

Abdul-Razzaq, K.S. and Dawood, A.A., 2021. Reinforcing Struts and Ties in Concrete Corbels. *ACI Structural Journal*, 118(4). DOI:10.14359/51732650

ACI Committee 318, 2019. *Building Code Requirements for Structural Concrete (ACI 318-19) and Commentary*. American Concrete Institute, Farmington Hills, MI, USA.

Abreu, I.C.D., Miranda, A.C.D.O., Lameiras, R.D.M. and Leite, C.H.D.O., 2024. Experimental results and limit load analysis by the strut-and-tie method (STM) in deep beams with notches and openings. *Revista IBRACON de Estruturas e Materiais*, 17(6), p.e17606. DOI:10.1590/s1983-41952024000600006

Adhikary, S.D., Li, B. and Fujikake, K., 2013. Strength and behavior in shear of reinforced concrete deep beams under dynamic loading conditions. *Nuclear Engineering and Design*, 259, pp.14-28. https://doi.org/10.1016/j.nucengdes.2013.02.016

Aguilar, V., Barnes, R.W. and Nowak, A., 2022. Strength reduction factors for ACI 318 strut-and-tie method for deep beams. *ACI Structural Journal*, 119(2), pp.103-112. DOI: 10.14359/51734332

Appa Rao, G. and Kunal, K., 2007. Shear strength of Reinforced Concrete deep beams. *Catania, Italy*, pp.671-5.

Arabzadeh, A., Hizaji, R. and Yang, T.Y., 2020. Experimentally studying and development of curved STM to predict the load capacity and failure mode of fixed-ended RC deep beams. *Structures*, 23, pp. 289-303. DOI:10.1016/j.istruc.2019.09.011

Arabzadeh, A., Rahaei, A.R. and Aghayari, R., 2009. A simple strut-and-tie model for prediction of ultimate shear strength of RC deep beams.

Bischoff, P.H. and Perry, S.H., 1991. Compressive behaviour of concrete at high strain rates. *Materials and structures*, 24(6), pp.425-450.

CEN (European Committee for Standardization), 2004. *Eurocode 2: Design of concrete structures—Part 1-1: General rules and rules for buildings*. Brussels, Belgium.

Collins, M.P. and Mitchell, D., 1986. Rational approach to shear design--the 1984 Canadian code provisions. *ACI Journal Proceedings*, 83(6), pp. 925-933.

Cusatis, G., 2011. Strain-rate effects on concrete behavior. *International Journal of Impact Engineering*, 38(4), pp.162-170. https://doi.org/10.1016/j.ijimpeng.2010.10.030

Erzar, B. and Forquin, P., 2010. An experimental method to determine the tensile strength of concrete at high rates of strain. *Experimental Mechanics*, 50(7), pp.941-955. DOI:10.1007/s11340-009-9284-z

Fan, S., Zhang, Y., Ma, Y.X. and Tan, K.H., 2022. Strut-and-tie and finite element modelling of unsymmetrically-loaded deep beams. *Structures*, 36, pp. 805-821. DOI:10.1016/j.istruc.2021.12.037

Fathi, H., Vaez, S.H., Zhang, Q. and Alavi, A.H., 2021. A new approach for crack detection in plate structures using an integrated extended finite element and enhanced vibrating particles system optimization methods. *Structures*, 29, pp. 638-651. DOI:10.1016/j.istruc.2021.12.037

Fujikake, K., Mori, K., Uebayashi, K., Ohno, T. and Mizuncr, J., 2000. Dynamic properties of concrete materials with high rates of tri-axial compressive loads. *WIT Transactions on The Built Environment*, 48. DOI:10.2495/SU000471

Grote, D.L., Park, S.W. and Zhou, M., 2001. Dynamic behavior of concrete at high strain rates and pressures: I. experimental characterization. *International journal of impact engineering*, 25(9), pp.869-886. https://doi.org/10.1016/S0734-743X(01)00020-3

Hussein, L.T. and Abbas, R.M., 2022. A semi-empirical equation based on the strut-and-tie model for the shear strength prediction of deep beams with multiple large web openings. *Engineering, Technology & Applied Science Research*, 12(2), pp.8289-8295. https://doi.org/10.48084/etasr.4743

International Federation for Structural Concrete (fib), 2010. *fib Model Code for Concrete Structures 2010*. Ernst & Sohn, Berlin, Germany. ISBN 978-2-88394-105-2.

Karimizadeh, H. and Arabzadeh, A., 2021. A STM-based analytical model for predicting load capacity of deep RC beams with openings. *Structures*, 34, pp. 1185-1200. https://doi.org/10.1016/j.istruc.2021.08.052

Kasilingam, S. and Khanna, M., 2024. Performance of Under Shear Reinforced Concrete Beams with varying Strength against Static and Impact Load. *Civil Engineering Infrastructures Journal*. https://doi.org/10.22059/ceij.2022.334953.1803

Kaveh, A., Hoseini Vaez, S.R., Hosseini, P. and Fathi, H., 2021. Crack detection with XFEM in plate structures using MDM operator. *International Journal of Optimization in Civil Engineering*, 11(2), pp.231-248.

Kelareh, M.F., Aghayari, R. and Roudsari, M.T., 2020. An experimental investigation into dispersion of compressive stress in isolated bottle-shaped struts with openings. *Structures*, 28, pp. 1857-1869. DOI:10.1016/j.istruc.2020.09.043

Kondalraj, R. and Rao, G.A., 2022. Efficiency of strut-and-tie model for design of reinforced concrete deep beams without web reinforcement. *ACI Structural Journal*, 119(3), pp.233-247. DOI:10.14359/51734494

Mabrouk, R.T., Mahmoud, M.A. and Kassem, M.E., 2022. Behavior of reinforced concrete deep beams with openings under vertical loads using strut and tie model. *Civil Engineering Journal*, 7, pp.148-170. DOI:10.28991/CEJ-SP2021-07-011

Malvar, L.J., Crawford, J.E., Wesevich, J.W. and Simons, D., 1997. A plasticity concrete material model for DYNA3D. *International journal of impact engineering*, 19(9-10), pp.847-873.

Megahed, K., 2024a. Prediction and reliability analysis of shear strength of RC deep beams. *Scientific Reports*, 14(1), p.14590. DOI:10.1038/s41598-024-64386-w

Megahed, K., 2024b. STM-based symbolic regression for strength prediction of RC deep beams and corbels. *Scientific Reports*, 14(1), p.25066. DOI:10.1038/s41598-024-74803-x

Mohammadizadeh, M.R., Esfandnia, F. and Khatibinia, M., 2023. Prediction of shear strength of reinforced concrete deep beams using neuro-fuzzy inference system and meta-heuristic algorithms. *Civil Engineering Infrastructures Journal*, 56(1), pp.137-157. https://doi.org/10.22059/ceij.2024.379538.2106

Mohammadi Rad, Z., Fazeli Kelareh, M., Fathi, H. and Aghayari, R., 2023. Investigating the Code Requirements and Influential Factors on the Determination of the Percentage of Maximum and Minimum Shear Reinforcement for Reinforced Concrete Deep Beams. *Iranian Journal of Science and Technology, Transactions of Civil Engineering*, 47(1), pp.281-304. https://doi.org/10.1007/s40996-022-00983-x

Mörsch, E., 1909. *Concrete-steel construction (der Eisenbetonbau)*. Engineering News Publishing Company, New York, USA.

Ozturk, B.M., 2003. *Seismic drift response of building structures in seismically active and near-fault regions*. Doctoral dissertation, Purdue University, West Lafayette, IN, USA.

Petersona, V., 2025. Strut and tie models for impulse-loaded reinforced concrete beams. *Shock & Impact Loads on Structures*, p.45. DOI:10.63959/silos15

Ramirez, J.A. and Breen, J.E., 1991. Evaluation of a modified truss-model approach for beams in shear. *ACI Structural Journal*, 88(5), pp.562-572.

Ritter, W., 1899. The Hennebique construction method ("Die Bauweise Hennebique"). *Schweizerische Bauzeitung*, 33(7), pp.41-61.

Sakalauskas, K. and Kaklauskas, G., 2023. Pure shear model for crack width analysis of reinforced concrete members. *Scientific Reports*, 13(1), p.13883. DOI:10.1038/s41598-023-41080-x

Schlaich, J. and Schäfer, K., 1991. Design and detailing of structural concrete using strut-and-tie models. *The Structural Engineer*, 69(6), pp.113-125.

Silveira, M.V., Bitencourt, L.A. and Das, S., 2022. A performance-based optimization framework applied to a classical STM-designed deep beam. *Structures*, 41, pp. 488-500. DOI:10.1016/j.istruc.2022.05.035

Thomas, J. and Ramadass, S., 2022. Introducing strut efficiency factor in the softened strut and tie model for the ultimate shear strength prediction of steel RC deep beams based on experimental study. *European Journal of Environmental and Civil Engineering*, 26(11), pp.5129-5166. DOI:10.1080/19648189.2021.1885500

Wu, K.C., Li, B. and Tsai, K.C., 2011. Residual axial compression capacity of localized blast-damaged RC columns. *International journal of impact engineering*, 38(1), pp.29-40. https://doi.org/10.1016/j.ijimpeng.2010.10.005

Yang, Z., Xiao, S. and Mao, L., 2025. Experimental Study on Dynamic Shear Behavior of RC Beams with Different Shear-Span Ratios at Various Loading Rates. *Journal of Structural Engineering*, 151(7), p.04025090. https://doi.org/10.1061/JSENDH.STENG-14384

Yi, W.J., Li, Y., Chen, H., Ma, Z.J., Zhou, K.J., Huang, Y. and Zhou, Y., 2022. Shear strength evaluation of RC D-Regions based on Single-Panel Strut-and-Tie model. *Engineering Structures*, 265, p.114500. DOI:10.1016/j.engstruct.2022.114500

Zhang, N. and Tan, K.H., 2007. Size effect in RC deep beams: Experimental investigation and STM verification. *Engineering structures*, 29(12), pp.3241-3254. https://doi.org/10.1016/j.engstruct.2007.09.001